

Hexacoordinate Phosphorus. 7. Synthesis and Characterization of Neutral Phosphorus(V) Compounds Containing Divalent Tridentate Diphenol Imine, Azo, and Thio Ligands

Chih Y. Wong, Robert McDonald, and Ronald G. Cavell*

Department of Chemistry, University of Alberta, Edmonton, AB, Canada T6G 2G2

Received June 15, 1995[⊗]

The reactions of bis(trimethylsilyl)ated forms of the Schiff base ligands *N*-(2-hydroxyphenyl)salicylideneamine $\{(\text{HO})\text{C}_6\text{H}_4\text{N}(\text{CH})\text{C}_6\text{H}_4(\text{OH})\}$, *N*-(4-*tert*-butyl-2-hydroxyphenyl)salicylideneamine $\{(\text{HO})(\text{tBu})\text{C}_6\text{H}_3\text{N}(\text{CH})\text{C}_6\text{H}_4(\text{OH})\}$, *N*-(2-hydroxy-4-nitrophenyl)salicylideneamine $\{(\text{HO})(\text{O}_2\text{N})\text{C}_6\text{H}_3\text{N}(\text{CH})\text{C}_6\text{H}_4(\text{OH})\}$, and the structurally related ligand 2,2'-azophenol with halogeno- and (trifluoromethyl)halogenophosphoranes yield a series of neutral hexacoordinate phosphorus(V) compounds by means of trimethylsilyl halide elimination. In all of these cases the ligands chelate in a meridional conformation in which bicyclic five- and six-membered chelate rings are formed through structures containing two phenolic P–O bonds and one N–P bond. The hexacoordinate nature of these compounds is evidenced by their high-field ³¹P NMR chemical shifts and their characteristic *J*_{PF} coupling patterns and is further substantiated by the crystal structures of $\{\text{O}(\text{tBu})\text{C}_6\text{H}_3\text{N}(\text{CH})\text{C}_6\text{H}_4\text{O}\}\text{PCl}_3$ and $\{\text{OC}_6\text{H}_4\text{N}=\text{NC}_6\text{H}_4\text{O}\}\text{PF}_3$. Crystal data for $\{\text{O}(\text{tBu})\text{C}_6\text{H}_3\text{N}(\text{CH})\text{C}_6\text{H}_4\text{O}\}\text{PCl}_3$: triclinic, space group *P*1̄ (No. 2), *a* = 11.167(1) Å, *b* = 15.684(1) Å, *c* = 17.047(2) Å, *V* = 2840(1) Å³, *Z* = 2. Final *R* and *R*_w values were 0.051 and 0.079, respectively. Crystal data for $\{\text{OC}_6\text{H}_4\text{N}=\text{NC}_6\text{H}_4\text{O}\}\text{PF}_3$: monoclinic, space group *P*2₁/*c* (No. 14), *a* = 6.9393(8) Å, *b* = 12.450(2) Å, *c* = 13.907(2) Å, *V* = 1190.7(6) Å³, *Z* = 4. Final *R* and *R*_w values were 0.045 and 0.056, respectively. The molecular structures of $\{\text{O}(\text{tBu})\text{C}_6\text{H}_3\text{N}(\text{CH})\text{C}_6\text{H}_4\text{O}\}\text{PCl}_3$ and $\{\text{OC}_6\text{H}_4\text{N}=\text{NC}_6\text{H}_4\text{O}\}\text{PF}_3$ show that in both cases the Schiff base ligand chelates occupy the meridional plane about the six-coordinate phosphorus atom. In the case of $\{\text{OC}_6\text{H}_4\text{N}=\text{NC}_6\text{H}_4\text{O}\}\text{PF}_3$ the equivalent nitrogen atoms in the chelate rings are disordered to form half-occupancy pairs. The silylated form of the related thiobis(phenol), 2,2'-thiobis(4,6-*tert*-butylphenol), reacted similarly with pentavalent halides to form the six-coordinate complex $\{[2\text{-O-3,5-(tBu)}_2\text{C}_6\text{H}_2]_2\text{S}\}\text{PCl}_3$ which was also verified by a crystal structure. Crystal data for $\{[2\text{-O-3,5-(tBu)}_2\text{C}_6\text{H}_2]_2\text{S}\}\text{PCl}_3$: monoclinic *P*2₁/*n*, *a* = 13.989(2), *b* = 13.594(2), *c* = 16.483(2) Å, β = 97.98(2)°, *V* = 3104(2) Å³, *Z* = 4; final *R* and *R*_w values were 0.039 and 0.052, respectively. In contrast to the above six coordinate complexes, this compound possesses a facial structure in which two phenoxy substituents form planar chelates centered on the bridging sulfur and intersecting at the P–S axis. The P–S bond length, 2.331(1) Å, is slightly shorter than has been previously observed in the example wherein the ligand possesses two *tert*-butyl groups and the phosphorus carries three OCH₂CF₃ substituents indicating stronger interaction between P and S in the present case.

Introduction

We have previously described the synthesis and characterization of various neutral hexacoordinate phosphorus(V) compounds utilizing the chelate effect of one monovalent bidentate ligand to form a four-, a five-, or a six-membered chelate ring. Examples include the carbamates and thiocarbamates,¹ 8-oxyquinolates,² acetylacetonates,³ amidinates,⁴ 2-oxypyridine, and related analogues.⁵ In all cases, formation of the hexacoordinate phosphorus(V) center is stabilized by rendering the phosphorus(V) center highly acidic using electron-withdrawing substituents such as F, Cl, or CF₃. Holmes and co-workers⁶ have described a series of pentacoordinate systems derived from trifluoroethyl phosphites with bridged 2,2'-diphenols which form eight-membered cyclic systems and which in some cases show internal coordination to form two pentacycles. Herein we

describe the formation of a series of neutral hexacoordinate phosphorus(V) compounds obtained from simple halogeno and trifluoromethyl P(V) precursors using tridentate bivalent ligands *N*-(2-hydroxyphenyl)salicylideneamine $\{(\text{HO})\text{C}_6\text{H}_4\text{N}(\text{CH})\text{C}_6\text{H}_4(\text{OH})\}$, *N*-(4-*tert*-butyl-2-hydroxyphenyl)salicylideneamine $\{(\text{HO})(\text{tBu})\text{C}_6\text{H}_3\text{N}(\text{CH})\text{C}_6\text{H}_4(\text{OH})\}$, *N*-(2-hydroxy-4-nitrophenyl)salicylideneamine $\{(\text{HO})(\text{O}_2\text{N})\text{C}_6\text{H}_3\text{N}(\text{CH})\text{C}_6\text{H}_4(\text{OH})\}$, the related ligand 2,2'-azophenol $\{(\text{HO})\text{C}_6\text{H}_4\text{N}=\text{NC}_6\text{H}_4(\text{OH})\}$ and 2,2'-thiobis(4,6-bis(*tert*-butyl)phenol), 2,2'- $\{(\text{HO})\text{-4,6-(tBu)}_2\text{C}_6\text{H}_2\}_2\text{S}$ depicted in (Figure 1). The first two systems form a bicyclic compounds containing a five- and a six-membered chelate ring bound in the meridional conformation. The latter forms two chelate rings bound in a bifacial conformation.

Experimental Section

1. General Procedures. All manipulations were carried out either in a vacuum or under an atmosphere of dry argon. The (trifluoromethyl)phosphoranes (CF₃)PCl₄, (CF₃)₂PCl₃, (CF₃)₃PCl₂, (CF₃)PF₄, and (CF₃)₂PF₃ were prepared according to published methods.⁷ Solvents were dried and distilled before use. Solution NMR spectra were recorded with Bruker WP200 and Bruker WP400 spectrometers.

[⊗] Abstract published in *Advance ACS Abstracts*, December 1, 1995.

- (1) Cavell, R. G.; Vande Griend, L. *Inorg. Chem.*: (a) **1986**, 25, 4699; (b) **1983**, 22, 2066.
- (2) John, K. P.; Schmutzler, R.; Sheldrick, W. S. *J. Chem. Soc., Dalton Trans.* **1974**: (a) 1841; (b) 2466.
- (3) Brown, N. M. D.; Bladon, P. J. *J. Chem. Soc., Chem. Commun.* **1966**, 304. Sheldrick, W. S.; Hewson, M. J. C. *Z. Naturforsch., B: Anorg. Chem.* **1978**, 33B, 834. Burford, N.; Kennepohl, D. K.; Cowie, M.; Ball, R. G.; Cavell, R. G. *Inorg. Chem.* **1987**, 26, 650.
- (4) Kennepohl, D. K.; Santarsiero, B. D.; Cavell, R. G. *Inorg. Chem.* **1990**, 29, 5081.
- (5) Kennepohl, D. K.; Pinkerton, A. A.; Lee, Y. F.; Cavell, R. G. *Inorg. Chem.* **1990**, 29, 5088.

- (6) Holmes, R. R.; Prakasha, T. K.; Day, R. O. *Inorg. Chem.* **1993**, 32, 4360. (b) Prakasha, T. K.; Day, R. O.; Holmes, R. R. *Inorg. Chem.* **1992**, 31, 1913. (c) Prakasha, T. K.; Day, R. O.; Holmes, R. R. *Inorg. Chem.* **1992**, 31, 3391. (d) Prakasha, T. K.; Day, R. O.; Holmes, R. R. *J. Am. Chem. Soc.*, **1993**, 115, 2690. (e) Prakasha, T. K.; Day, R. O.; Holmes, R. R. *Inorg. Chem.* **1992**, 31, 725.

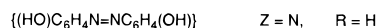
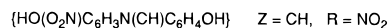
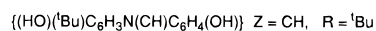
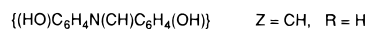
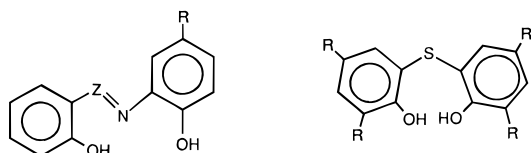


Figure 1. Structures of the ligands.

CPMAS NMR spectra were recorded with a Bruker WP300 spectrometer. Chemical shifts are quoted relative to $Si(CH_3)_4$ for the 1H nucleus, $CFCl_3$ for the ^{19}F nucleus, and 85% H_3PO_4 for the ^{31}P nucleus. For all the nuclei, negative chemical shifts represent shifts upfield (lower frequency). Mass spectra were recorded with an AEI MS-12 spectrometer operating at an ionizing voltage of 70 eV. Melting points were determined on samples sealed in melting point capillaries and are uncorrected. Chemical analyses were determined by the Department of Chemistry, University of Alberta, and by Schwarzkopf Microanalytical Laboratory, Woodside, NY.

2. Preparation of the Ligands. The Schiff base ligands were prepared by mixing (1:1) the appropriate 2-aminophenol with salicylaldehyde in hot ethanol. The solution was cooled to 0 °C overnight to crystallize the adduct. 2,2'-Azophenol was obtained from Aldrich and used without further purification. The sulfur ligand, 2,2'-thiobis(4,6-bis(*tert*-butyl)phenol) was prepared as described.^{6d} Silylation of the protonated ligands was carried out by refluxing the ligands with excess hexamethyldisilazane under Ar. The product was then purified by vacuum distillation. As an example, the preparation of *N*-(4-*tert*-butyl-2-hydroxyphenyl)salicylideneamine, $\{(HO)(t-Bu)C_6H_3N(CH)C_6H_4(OH)\}$, follows. A sample of 2-amino-4-*tert*-butylphenol (10.09 g, 61.1 mmol) was dissolved in ethanol (100 mL) and salicylaldehyde (6.4 mL, 61.3 mmol) was added dropwise. The mixture was heated and stirred for 2 h. An orange brown crystalline product was obtained on cooling. The crystals were filtered, washed with a little cold ethanol and dried *in vacuo*. Yield: 10.57 g, 64%. 1H NMR (200 MHz, $CDCl_3$) δ : 1.32 (9H, s, *t*-Bu), 6.9–7.5 (7H, m, Ar), 8.66 (1H, s, N=CH).

Preparation of Silylated Ligands, e.g. $(Me_3SiO)(t-Bu)C_6H_3N(CH)C_6H_4(OSiMe_3)$. Silylation was accomplished as follows: a sample of $\{(HO)(t-Bu)C_6H_3N(CH)C_6H_4(OH)\}$ (8.10 g, 30.1 mmol) was mixed with $(SiMe_3)_2NH$ (40 mL, 190 mmol) under Ar with stirring. The mixture was refluxed for 24 h and then the excess $(SiMe_3)_2NH$ was removed *in vacuo*. The crude product was vacuum distilled (145 °C, 0.2 mmHg) to give a light-orange viscous oil. Yield: 7.7 g, 62%. 1H NMR (200 MHz, $CDCl_3$) δ : 0.20 (9H, s, $SiMe_3$), 0.30 (9H, s, $SiMe_3$), 1.30 (9H, s, *t*-Bu), 6.8–8.2 (7H, m, Ar), 8.84 (1H, s, N=CH).

3. Preparation of the Pentavalent Phosphorus Derivatives. Synthesis of the hexacoordinate phosphorus(V) compounds from the silylated ligands (or in some cases the protonated form of the ligands) and the appropriate PX_5 afforded quantitative crude yields with respect to the starting silylated ligand. Recrystallized yields varied from 30% to 60%.

(a) Preparation of $\{N$ -(4-*tert*-Butylphen-2-oxy)salicylideneaminato}-trichlorophosphorus(V), $\{[(O)(t-Bu)C_6H_3N(CH)C_6H_4O]P(Cl)_3\}$. A sample of $\{(Me_3SiO)(t-Bu)C_6H_3N(CH)C_6H_4(OSiMe_3)\}$ (4.25 g, 10.3 mmol) was added dropwise to a stirred solution of PCl_5 (20.5 mL, 0.5 M in dichloromethane, 10.3 mmol) under Ar. The solvent was removed *in vacuo* after 24 h stirring at room temperature to leave a pale orange solid. A pure sample may be obtained by recrystallization from warm dichloromethane or acetonitrile. Mp: 250 °C dec, without melting. Anal. Calcd for $C_{17}H_{17}Cl_3NO_2P$: C, 50.46; H, 4.23; Cl, 26.28; N, 3.46; P, 7.65. Found: C, 49.94; H, 4.45; Cl, 25.13; N, 3.46; P, 7.24. MS

(*m/e* (relative intensity, % of strongest peak) [identity]): 403 (10) [M]; 368 (100) [M – Cl]; 333 (8) [M – 2Cl]; 298 (22) [M – 3Cl].

(b) Preparation of $\{N$ -(4-*tert*-Butylphen-2-oxy)salicylideneaminato}-trifluoromethyl)dichlorophosphorus(V), $\{(O)(t-Bu)C_6H_3N(CH)C_6H_4O\}P(CF_3)Cl_2$. A sample of $\{(Me_3SiO)(t-Bu)C_6H_3N(CH)C_6H_4(OSiMe_3)\}$ (0.20 g, 0.48 mmol) was dissolved in dichloromethane (2 mL) under Ar and degassed under vacuum. $(CF_3)PCl_4$ (0.14 g, 0.58 mmol) was condensed into the vessel at –196 °C and sealed. The vessel was allowed to warm to room temperature slowly overnight, and the reaction was allowed to proceed to completion for another 24 h at room temperature with occasional shaking. The volatile materials were removed *in vacuo* to leave a dark orange crystalline solid. A pure sample was obtained by recrystallization from warm acetonitrile (*ca.* 5 mL) as bright orange crystals. Mp: 272–276 °C dec. Anal. Calcd for $C_{18}H_{17}Cl_2F_3NO_2P$: C, 49.34; H, 3.91; Cl, 16.18; N, 3.20. Found: C, 48.46; H, 3.73; Cl, 16.03; N, 3.15. MS (*m/e* (relative intensity, % of strongest peak) [identity]): 437 (6) [M]; 402 (100) [M – Cl]; 383 (9) [$\{(O)(t-Bu)C_6H_3N(CH)C_6H_4O\}P(Cl)=CF_2$]; 368 (23) [$\{(O)(t-Bu)C_6H_3N(CH)C_6H_4O\}P(Cl)_2$]; 352 (26) [$\{(O)(t-Bu)C_6H_3N(CH)C_6H_4O\}PFCl$]; 336 (53) [$\{(O)(t-Bu)C_6H_3N(CH)C_6H_4O\}PF_2$]; 314 (33) [$\{(O)(t-Bu)C_6H_3N(CH)C_6H_4O\}P=O$]; 298 (24) [$\{(O)(t-Bu)C_6H_3N(CH)C_6H_4O\}P$].

(c) Preparation of $\{N$ -(Phen-2-oxy)salicylideneaminato}bis(trifluoromethyl)chlorophosphorus(V), $\{OC_6H_4N(CH)C_6H_4O\}P(CF_3)_2Cl$. A sample of $\{(Me_3SiO)C_6H_4N(CH)C_6H_4(OSiMe_3)\}$ (0.43 g, 1.20 mmol) was dissolved in acetonitrile (3 mL) under Ar and degassed under vacuum. $(CF_3)_2PCl_3$ (0.42 g, 1.53 mmol) was condensed into the vessel at –196 °C and sealed. The vessel was allowed to warm to room temperature slowly overnight and the reaction was completed in another 24 h at 50–55 °C with occasional shaking. The volatile materials were removed *in vacuo* to leave a dark orange solid. A pure sample may be obtained by recrystallization from warm acetonitrile (*ca.* 15 mL) to give bright orange-yellow crystals. Mp: 205 °C, dec, without melting. Anal. Calcd for $C_{15}H_9ClF_6NO_2P$: C, 43.34; H, 2.18; Cl, 8.53; N, 3.37. Found: C, 43.24; H, 1.99; Cl, 8.51; N, 3.39. MS (*m/e* (relative intensity, % of strongest peak) [identity]): 415 (9) [M]; 380 (47) [M – Cl]; 346 (31) [M – CF_3]; 330 (38) [$\{OC_6H_4N(CH)C_6H_4O\}PF(CF_3)$]; 296 (12) [$\{OC_6H_4N(CH)C_6H_4O\}PFCl$]; 280 (100) [$\{OC_6H_4N(CH)C_6H_4O\}PF_2$]; 258 (27) [$\{OC_6H_4N(CH)C_6H_4O\}P=O$]; 242 (54) [$\{OC_6H_4N(CH)C_6H_4O\}P$].

(d) Preparation of $\{N$ -(Phen-2-oxy)salicylideneaminato}(trifluoromethyl)difluorophosphorus(V), $\{OC_6H_4N(CH)C_6H_4O\}P(CF_3)F_2$. A sample of $(Me_3SiO)C_6H_4N(CH)C_6H_4(OSiMe_3)$ (0.34 g, 0.95 mmol) was dissolved in acetonitrile (3 mL) under Ar and degassed under vacuum. Approximately 1.70 mmol $(CF_3)PF_4$ was condensed into the vessel at –196 °C and sealed. The vessel was allowed to warm to room temperature slowly overnight. The volatile materials were removed *in vacuo*, and the yellow solid was transferred to a round bottom flask and refluxed overnight in acetonitrile (20 mL). Bright yellow needles crystallized upon cooling. Mp: 210 °C dec, without melting. Anal. Calcd for $C_{14}H_9F_5NO_2P$: C, 48.15; H, 2.60; N, 4.01. Found: C, 48.15; H, 2.41; N, 4.06. MS (*m/e* (relative intensity, % of strongest peak) [identity]): 349 (52) [M]; 330 (3) [M – F]; 281 (100) [M – CF_3]; 260 (53) [$\{OC_6H_4N(CH)C_6H_4O(OH)P\}$]; 211 (13) [$\{OC_6H_4N(CH)C_6H_4O\}P$].

(e) Preparation of $\{N$ -(4-*tert*-Butylphen-2-oxy)salicylideneaminato}-trifluorophosphorus(V), $\{(O)(t-Bu)C_6H_3N(CH)C_6H_4O\}PF_3$. A sample of $(Me_3SiO)(t-Bu)C_6H_3N(CH)C_6H_4(OSiMe_3)$ (0.39 g, 0.94 mmol) was dissolved in dichloromethane (2 mL) under Ar and degassed under vacuum. Approximately 0.94 mmol $PF_5(g)$ was condensed into the vessel at –196 °C and sealed. The vessel was allowed to warm to room temperature slowly overnight, and the reaction was completed in another 24 h at room temperature with occasional shaking. The volatile materials were removed *in vacuo* to leave an orange crystalline solid. A pure sample was obtained by recrystallization from warm dichloromethane (*ca.* 1 mL) as bright orange crystals. Mp: 216–220 °C. Anal. Calcd for $C_{17}H_{17}F_3NO_2P$: C, 57.47; H, 4.82; F, 16.04; N, 3.94; P, 8.78. Found: C, 56.95; H, 4.98; F, 15.91; N, 4.02; P, 8.32. MS (*m/e* (relative intensity, % of strongest peak) [identity]): 355 (41) [M]; 340 (100) [M – CH_3].

(7) Emeleus, H. J.; Haszeldine, R. N.; Paul, R. C. *J. Chem. Soc.* **1955**, 563. Bennett, F. W.; Emeleus, H. J.; Haszeldine, R. N. *J. Chem. Soc.* **1953**, 1565. Mahler, W. *Inorg. Chem.* **1963**, *2*, 230. Volbach, W.; Ruppert, I. *Tetrahedron Lett.* **1983**, *24*, 5509. Schäfer, S. Dissertation, Bonn, Germany, 1988.

Table 1. Crystallographic Data for **A**, $3\{[O(\text{t-Bu})C_6H_3N(\text{CH})C_6H_4O]PCl_3 \cdot 0.5CH_3CN\}$, **B**, $\{OC_6H_4N=NC_6H_4O\}PF_3$ and **C**, $\{[2-O-3,5-(\text{t-Bu})_2C_6H_2]_2S\}PCl_3$

	A	B	C
formula	$C_{52}H_{52.5}Cl_9N_{3.5}O_6P_3$	$C_{12}H_8F_3N_2O_2P$	$C_{28}H_{40}Cl_3O_2PS$
color	orange	deep red-orange	pale yellow
mounting	glass capillary	glass fiber	glass capillary
fw	1234.51	300.18	578.03
cryst size (mm)	$0.66 \times 0.33 \times 0.21$	$0.87 \times 0.33 \times 0.15$	$0.87 \times 0.54 \times 0.44$
cryst syst	triclinic	monoclinic	monoclinic
space group ^a	$P\bar{1}$ (No. 2)	$P2_1/c$ (No. 14)	$P2_1/n^b$
unit cell params			
<i>a</i> (Å)	11.167(1)	6.9393(8)	13.989(2)
<i>b</i> (Å)	15.684(1)	12.450(2)	13.594(2)
<i>c</i> (Å)	17.047(2)	13.907(2)	16.483(3)
α (deg)	92.15(1)		
β (deg)	104.098(9)	97.67(2)	97.98(2)
γ (deg)	100.19(1)		
<i>V</i> (Å ³)	2840(1)	1190.7(6)	3104(2)
<i>Z</i>	2	4	4
ρ_{calcd} (g cm ⁻³)	1.443	1.674	1.237
μ (cm ⁻¹)	5.79	2.64	4.33
diffractometer ^c	Enraf-Nonius CAD4	Enraf-Nonius CAD4	Enraf-Nonius CAD4
radiation (λ [Å])	Mo K α (0.710 73)	Mo K α (0.710 73)	Mo K α (0.710 73)
temp (°C)	-50	-50	-50
scan type	$\theta-2\theta$	$\theta-2\theta$	$\theta-2\theta$
max 2θ (deg)	50.0	50.0	50.0
tot. no. of data colld	10319	2292	5884
no of indep reflns	9895	2201	5677
no. of observns ($I \geq 3\sigma(I)$) (<i>NO</i>)	6274	1348	3941
structure solution method	direct methods ^d	direct methods ^d	direct methods ^d
refinement method	full-matrix on <i>F</i> ^e	full-matrix on <i>F</i> ^e	full-matrix on <i>F</i> ^e
abs cor method	DIFABS ^f	DIFABS ^f	DIFABS ^f
range of abs. cor factors	1.1195-0.7946	1.4416-0.6721	1.0776-0.8241
no. of params (<i>NV</i>)	661	199	316
goodness-of-fit (<i>S</i>) ^g	2.314	1.723	1.700
final <i>R</i> indices ^h			
<i>R</i>	0.051	0.045	0.039
<i>R</i> _w	0.079	0.056	0.052

^a *International Tables for X-Ray Crystallography*; Kynoch: Birmingham, England, 1969; Vol. I. ^b A non-standard setting of $P2_1/c$ (No. 14).

^c The diffractometer programs are those supplied by Enraf-Nonius for operating the CAD4F diffractometer, with some local modifications by Dr. R. G. Ball of the University of Alberta Structure Determination Laboratory. ^d Sheldrick, G. M. *Acta Crystallogr.* **1990**, *A46*, 467. ^e *Structure Determination Package*, Version 3 (Enraf-Nonius, Delft, The Netherlands, 1985) adapted for a Sun Microsystems SPARCstation 1+ computer, and several locally written programs by Dr. R. G. Ball. ^f Walker, N.; Stuart, D. *Acta Crystallogr.* **1983**, *A39*, 158. ^g $S = [\sum w(|F_o| - |F_c|)^2 / (NO - NV)]^{1/2}$ ($w = 4F_o^2/\sigma^2(F_o^2)$). ^h $R = \sum ||F_o| - |F_c|| / \sum |F_o|$; $R_w = [\sum w(|F_o| - |F_c|)^2 / \sum wF_o^2]^{1/2}$.

(f) Preparation of $\{N-(4\text{-Nitrophenoxy})\text{salicylideneaminato}\}$ -trifluorophosphorus(V), $\{O(O_2N)C_6H_3N(\text{CH})C_6H_4O\}PF_3$. The preparation was carried out in a similar fashion to that described in section 3(d) above. A pure sample was obtained by recrystallization from hot acetonitrile (*ca.* 10 mL) as light yellow crystals. Mp: 220–230 °C dec without melting. Anal. Calcd for $C_{13}H_8F_3N_2O_4P$: C, 45.37; H, 2.34; N, 8.14. Found: C, 45.21; H, 2.33; N, 8.13. MS (*m/e* (relative intensity, % of strongest peak) [identity]): 344 (100) [M]; 256 (15) [$\{O(O_2N)C_6H_3N(\text{CH})C_6H_4O\}$].

(g) Preparation of (2,2'-Azophenoxy)trifluorophosphorus(V), $\{OC_6H_4N=NC_6H_4O\}PF_3$. The preparation was carried out in a similar fashion to that described in section 3(d) above. A pure sample was obtained by recrystallization from hot acetonitrile (*ca.* 10 mL) as dark red crystals. Mp: 180 °C, dec, without melting. Anal. Calcd for $C_{12}H_8F_3N_2O_2P$: C, 48.02; H, 2.69; N, 9.33. Found: C, 48.23; H, 2.71; N, 9.33. MS (*m/e* (relative intensity, % of strongest peak) [identity]): 300 (100) [M]; 281 (2) [M - F].

(h) Preparation of (2,2'-Azophenoxy)(trifluoromethyl)difluorophosphorus(V), $\{OC_6H_4N=NC_6H_4O\}P(\text{CF}_3)_2$. Mp: 140–150 °C dec, and melting *ca.* 160 °C. No satisfactory analyses were obtained for this compound. MS (*m/e* (relative intensity, % of strongest peak) [identity]): 350 (32) [M]; 331 (3) [M - F]; 281 (100) [M - CF₃]; 300 (3) [$\{OC_6H_4N=NC_6H_4O\}PF_3$]. Partial separation of isomers was achieved by fractional recrystallization: The *cis*-isomer was isolated by repeated recrystallization from acetonitrile. Most of the *cis*-isomer was depleted after several crops and the residue was evaporated to dryness and washed with a little dichloromethane to leave mainly the *trans*-isomer. This was recrystallized from hexane/dichloromethane (10:1).

(i) Preparation of Thiobis(3,5-bis(*tert*-butyl)-*o*-phenylenedioxy)-trichlorophosphorus(V), $\{[2-O-3,5-(\text{t-Bu})_2C_6H_2]_2S\}PCl_3$. Reaction of $\{2-(\text{HO})-3,5-(\text{t-Bu})_2C_6H_2\}_2S$ (1.17 g, 2.64 mmol), and 2.65 mmol PCl_5 in CH_2Cl_2 (10 mL) proceeded smoothly during an overnight reflux. The product was a pale yellow-orange solid. δ -133.9 ppm. Anal. Calcd for $C_{28}H_{40}Cl_3O_2PS$: C, 58.18; H, 6.97; Cl, 18.40. Found: C, 58.35; H, 6.88; Cl, 18.45.

X-ray Data Collection^{8,9} for $\{O(\text{t-Bu})C_6H_3N(\text{CH})C_6H_4O\}PCl_3$, $\{OC_6H_4N=NC_6H_4O\}PF_3$ and $\{[2-O-3,5-(\text{t-Bu})_2C_6H_2]_2S\}PCl_3$. Details of the crystallographic analyses are given in Table 1. In all cases the structures were determined at low temperatures (Table 1). Collection and refinement programs, absorption and correction factors, and other parameters are given in Table 1. In each case refinement of hydrogen atoms of the complex was accomplished by generation of each H atom at an idealized calculated position by assuming a C-H bond length of 0.95 Å and the appropriate sp² or sp³ geometry. All hydrogen atoms of the complex were then included in the refinement calculation cycle with fixed, isotropic Gaussian displacement parameters 1.2 times those of the attached atoms, and were constrained to "ride" on the attached

(8) X-ray crystallographic studies were carried out by Dr. R. McDonald at the Structure Determination Laboratory, Department of Chemistry, University of Alberta. Inquiries regarding the crystallographic results should be directed to the above address quoting report reference codes SDL:RGC9303 for $\{O(\text{t-Bu})C_6H_3N(\text{CH})C_6H_4O\}PCl_3$, SDL:RGC9307 for $\{OC_6H_4N=NC_6H_4O\}PF_3$, and SDL:RGC9306 for $\{[2-O-3,5-(\text{t-Bu})_2C_6H_2]_2S\}PCl_3$ respectively.

(9) We thank Prof. M. Cowie of this department for allowing use of his CAD4 diffractometer for collection of data used in the structure determination of $\{O(\text{t-Bu})C_6H_3N(\text{CH})C_6H_4O\}PCl_3$.

Table 2. Atomic Correspondences for the Three Independent Molecules in $\{O(\text{tBu})C_6H_3N(\text{CH})C_6H_4O\}PCl_3$

molecule 1	molecule 2	molecule 3
P(1)	P(2)	P(3)
Cl(11)	Cl(21)	Cl(31)
Cl(12)	Cl(22)	Cl(32)
Cl(13)	Cl(23)	Cl(33)
O(11)	O(21)	O(31)
O(12)	O(22)	O(32)
N(1)	N(2)	N(3)
C(11)–C(23) ^a	C(31)–C(43)	C(51)–C(63)
C(24)–C(27) ^b	C(44)–C(47)	C(64)–C(67)

^a Ring framework atoms. ^b *tert*-Butyl group.

Table 3. Atomic Coordinates and Equivalent Isotropic Displacement Parameters for the Important Atoms of the Three Independent Molecules^a of $\{O(\text{tBu})C_6H_3N(\text{CH})C_6H_4O\}PCl_3$

atom	<i>x</i>	<i>y</i>	<i>z</i>	<i>B</i> _{eq} ^b , Å ²
Cl(11)	0.1520(2)	−0.2401(1)	0.5178(1)	4.15(5)*
Cl(12)	0.1561(2)	−0.2921(1)	0.3427(1)	3.06(4)*
Cl(13)	0.3787(2)	−0.1411(1)	0.3580(1)	3.38(5)*
Cl(21)	0.3537(1)	0.1829(1)	−0.06424(9)	2.65(4)*
Cl(22)	0.1696(1)	0.0242(1)	−0.1644(1)	2.58(4)*
Cl(23)	0.3209(2)	0.0379(1)	−0.29160(9)	2.56(4)*
Cl(31)	0.4188(2)	−0.3899(1)	0.0914(1)	3.15(4)*
Cl(32)	0.2370(1)	−0.4106(1)	0.1991(1)	2.66(4)*
Cl(33)	0.2061(2)	−0.6077(1)	0.1764(1)	2.80(4)*
P(1)	0.2594(2)	−0.1962(1)	0.4336(1)	2.09(4)*
P(2)	0.3306(1)	0.1064(1)	−0.17717(9)	1.76(4)*
P(3)	0.3114(1)	−0.4971(1)	0.1369(1)	2.06(4)*
O(11)	0.1580(4)	−0.1337(3)	0.3973(3)	3.2(1)*
O(12)	0.3572(4)	−0.2640(3)	0.4655(2)	2.5(1)*
O(21)	0.2412(4)	0.1729(3)	−0.2240(2)	2.4(1)*
O(22)	0.4169(3)	0.0395(2)	−0.1265(2)	1.8(1)*
O(31)	0.1918(4)	−0.5014(3)	0.0559(2)	2.5(1)*
O(32)	0.4301(4)	−0.4908(3)	0.2207(2)	2.5(1)*
N(1)	0.3612(4)	−0.1141(3)	0.5154(3)	1.9(1)*
N(2)	0.4798(4)	0.1747(3)	−0.1865(3)	1.5(1)*
N(3)	0.3873(4)	−0.5737(3)	0.0870(3)	2.1(1)*
C(11)	0.1482(5)	−0.0533(4)	0.4232(3)	2.1(1)*
C(16)	0.2417(5)	−0.0010(4)	0.4852(3)	1.9(1)*
C(17)	0.3467(5)	−0.0345(4)	0.5284(3)	2.0(1)*
C(18)	0.4595(5)	−0.1514(4)	0.5636(3)	2.0(1)*
C(23)	0.4499(6)	−0.2353(4)	0.5335(4)	2.2(2)*
C(31)	0.2629(6)	0.2265(4)	−0.2824(4)	2.1(2)*
C(36)	0.3840(5)	0.2592(4)	−0.2892(3)	2.0(1)*
C(37)	0.4900(5)	0.2344(4)	−0.2360(3)	1.8(1)*
C(38)	0.5836(5)	0.1461(4)	−0.1384(3)	1.8(1)*
C(43)	0.5443(5)	0.0697(4)	−0.1058(3)	1.8(1)*
C(51)	0.1872(5)	−0.5187(4)	−0.0233(4)	2.4(2)*
C(56)	0.2652(6)	−0.5699(4)	−0.0473(4)	2.3(2)*
C(57)	0.3586(6)	−0.5988(4)	0.0108(4)	2.3(2)*
C(58)	0.4869(6)	−0.5970(4)	0.1462(4)	2.2(2)*
C(63)	0.5064(6)	−0.5503(4)	0.2193(4)	2.4(2)*
C(90)	0.200(2)	0.488(1)	0.404(1)	7.1(5)
C(91)	0.313(2)	0.504(1)	0.421(1)	6.2(5)
C(92)	0.428(2)	0.507(1)	0.457(1)	5.8(4)

^a Atomic correspondences are given in Table 2. ^b Values for anisotropically-refined atoms are marked with an asterisk. Displacement parameters for the anisotropically refined atoms are given in the form of the equivalent isotropic Gaussian displacement parameter, *B*_{eq}, defined as $4/3[a^2\beta_{11} + b^2\beta_{22} + c^2\beta_{33} + ab(\cos \gamma)\beta_{12} + ac(\cos \beta)\beta_{13} + bc(\cos \alpha)\beta_{23}]$.

atoms. Final refinement parameters are given in Table 1, and in all cases the highest peak in the final difference Fourier map was small and without chemical significance. The structures are illustrated as ORTEP¹⁰ plots.

In the case of $\{O(\text{tBu})C_6H_3N(\text{CH})C_6H_4O\}PCl_3$ the asymmetric crystal unit was found to consist of three crystallographically-independent molecules of the complex and a half-occupancy molecule of acetonitrile,

Table 4. Selected Important Interatomic Bond Lengths (Å) for $\{O(\text{tBu})C_6H_3N(\text{CH})C_6H_4O\}PCl_3^a$

Cl(11)–P(1)	2.143(2)	O(22)–C(43)	1.370(5)
Cl(12)–P(1)	2.081(2)	O(31)–C(51)	1.353(5)
Cl(13)–P(1)	2.167(2)	O(32)–C(63)	1.373(5)
Cl(21)–P(2)	2.165(2)	N(1)–C(17)	1.304(5)
Cl(22)–P(2)	2.082(2)	N(1)–C(18)	1.431(5)
Cl(23)–P(2)	2.161(2)	N(2)–C(37)	1.291(5)
Cl(31)–P(3)	2.169(2)	N(2)–C(38)	1.402(5)
Cl(32)–P(3)	2.091(2)	N(3)–C(57)	1.288(5)
Cl(33)–P(3)	2.144(2)	N(3)–C(58)	1.420(5)
P(1)–O(11)	1.650(3)	C(16)–C(17)	1.421(5)
P(1)–O(12)	1.669(3)	C(18)–C(19)	1.397(5)
P(1)–N(1)	1.864(3)	C(18)–C(23)	1.370(6)
P(2)–O(21)	1.663(3)	C(36)–C(37)	1.429(5)
P(2)–O(22)	1.672(3)	C(38)–C(39)	1.389(5)
P(2)–N(2)	1.860(3)	C(38)–C(43)	1.386(5)
P(3)–O(31)	1.660(3)	C(51)–C(56)	1.403(6)
P(3)–O(32)	1.683(3)	C(56)–C(57)	1.404(6)
P(3)–N(3)	1.877(3)	C(58)–C(59)	1.402(6)
O(11)–C(11)	1.351(5)	C(58)–C(63)	1.371(6)
O(12)–C(23)	1.353(5)	C(90)–C(91)	1.20(2)
O(21)–C(31)	1.365(5)	C(91)–C(92)	1.27(2)

^a Atomic correspondences for independent molecules given in Table 2.

Table 5. Selected Interatomic Angles (deg) for One of the Three Equivalent Molecules in the Structure of $\{O(\text{tBu})C_6H_3N(\text{CH})C_6H_4O\}PCl_3^a$

Cl(11)–P(1)–Cl(12)	93.50(7)	C(13)–C(14)–C(15)	118.8(4)
Cl(11)–P(1)–Cl(13)	174.03(8)	C(14)–C(15)–C(16)	120.5(4)
Cl(11)–P(1)–O(11)	89.8(1)	C(11)–C(16)–C(15)	119.1(4)
Cl(11)–P(1)–O(12)	90.7(1)	C(11)–C(16)–C(17)	120.4(4)
Cl(11)–P(1)–N(1)	88.0(1)	C(15)–C(16)–C(17)	120.5(4)
Cl(12)–P(1)–Cl(13)	92.46(6)	N(1)–C(17)–C(16)	123.4(4)
Cl(12)–P(1)–O(11)	88.2(1)	N(1)–C(18)–C(19)	128.0(4)
Cl(12)–P(1)–O(12)	88.3(1)	N(1)–C(18)–C(23)	109.8(4)
Cl(12)–P(1)–N(1)	176.1(1)	C(19)–C(18)–C(23)	122.1(4)
Cl(13)–P(1)–O(11)	90.2(1)	C(18)–C(19)–C(20)	118.6(4)
Cl(13)–P(1)–O(12)	89.7(1)	C(19)–C(20)–C(21)	118.4(4)
Cl(13)–P(1)–N(1)	86.1(1)	C(19)–C(20)–C(24)	121.5(4)
O(11)–P(1)–O(12)	176.4(2)	C(21)–C(20)–C(24)	119.8(4)
O(11)–P(1)–N(1)	95.4(1)	C(20)–C(21)–C(22)	122.8(4)
O(12)–P(1)–N(1)	88.1(1)	C(21)–C(22)–C(23)	117.8(4)
P(1)–O(11)–C(11)	131.5(3)	O(12)–C(23)–C(18)	116.4(4)
P(1)–O(12)–C(23)	115.7(3)	O(12)–C(23)–C(22)	123.3(4)
P(1)–N(1)–C(17)	126.2(3)	C(18)–C(23)–C(22)	120.3(4)
P(1)–N(1)–C(18)	109.6(3)	C(20)–C(24)–C(25)	112.1(3)
C(17)–N(1)–C(18)	124.1(3)	C(20)–C(24)–C(26)	108.4(3)
O(11)–C(11)–C(12)	116.7(4)	C(20)–C(24)–C(27)	109.8(4)
O(11)–C(11)–C(16)	122.5(4)	C(25)–C(24)–C(26)	109.5(4)
C(12)–C(11)–C(16)	120.8(4)	C(25)–C(24)–C(27)	108.1(4)
C(11)–C(12)–C(13)	118.8(4)	C(26)–C(24)–C(27)	108.8(4)
C(12)–C(13)–C(14)	122.0(4)	C(90)–C(91)–C(92)	163(2)

^a Atomic correspondences for independent molecules given in Table 2.

the crystallization solvent. The atom correspondences are given in Table 2. Three reflections were chosen as intensity and orientation standards, and these were remeasured after every 120 min of exposure time to check on crystal and electronic stability over the course of data collection; no appreciable decay was evident. All three atomic positions assigned to the acetonitrile molecule of crystallization were refined isotropically as half-occupancy carbon atoms. Attempts to refine either of the terminal atoms as nitrogen did not lead to an unambiguous assignment of one or the other as N atoms. For this reason the hydrogen atoms of solvent molecules were not included in the model. Anisotropic refinement of the three acetonitrile atoms was also unsuccessful. The complete positional and isotropic thermal parameters for $\{O(\text{tBu})C_6H_3N(\text{CH})C_6H_4O\}PCl_3$ are given in Table 3. Selected bond lengths and angles are given in Tables 4 and 5. Additional information is available as Supporting Information.

In the case of $\{OC_6H_4N=NC_6H_4O\}PF_3$, the positions of the nitrogen atoms of the $\{OC_6H_4N=NC_6H_4O\}$ subunit were found to be disordered and thus were modeled as two half-occupancy pairs. Three reflections

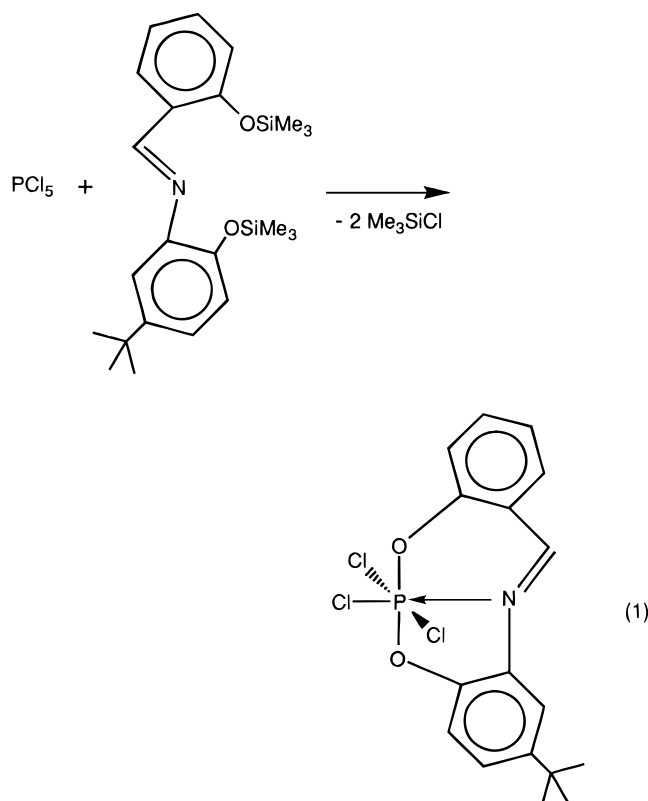
(10) Johnson, C. K. ORTEP; Report ORNL No. 5138, Oak Ridge National Laboratories: Oak Ridge, TN, 1976.

were chosen as intensity and orientation standards, and these were remeasured after every 120 min of exposure time to check on crystal and electronic stability over the course of data collection; no appreciable decay was evident. Complete positional and isotropic thermal parameters for $\{\text{OC}_6\text{H}_4\text{N}=\text{NC}_6\text{H}_4\text{O}\}\text{PF}_3$ are given in Table 6 and selected bond lengths and angles in Tables 7 and 8. Additional information is available as Supporting Information.

The structural determination of *fac*- $\{(2\text{-O-3,5-}(\text{t-Bu})_2\text{C}_6\text{H}_2)_2\text{S}\}\text{PCl}_3$ was straightforward however monitoring the intensity of three reflections for intensity and orientation standards at 120 min intervals revealed an average (linear) decrease in intensity of 11.9% over the time span of data collection, thus a linear decay correction was applied to the data. Complete positional and isotropic thermal parameters for *fac*- $\{(2\text{-O-3,5-}(\text{t-Bu})_2\text{C}_6\text{H}_2)_2\text{S}\}\text{PCl}_3$ are given in Table 9 and selected bond lengths and angles are given in Tables 10 and 11. Additional information is available as Supporting Information.

Results and Discussion

The silylated derivatives of the Schiff base ligands react readily with halogenophosphoranes to give high yields of the neutral hexacoordinate phosphorus(V) compounds *via* the elimination of 2 equiv of Me_3SiCl or Me_3SiF (e.g., eq 1).



The use of silylated ligands as opposed to the protonated analogues alleviates the problems that often arise due to side reactions caused by the byproducts, HCl and HF, as observed for systems described previously.⁵

The geometry of the ligand is such that when coordinated it produces a highly delocalized system which enhances stability. Formation of a five- and a six-membered bicyclic chelate utilizing a ONO donor set for these ligands has been previously demonstrated for metal ions such as vanadium(IV) and -(V)¹¹ and manganese(IV) and -(V).¹²

Table 6. Atomic Coordinates and Equivalent Isotropic Displacement Parameters for $\{\text{OC}_6\text{H}_4\text{N}=\text{NC}_6\text{H}_4\text{O}\}\text{PF}_3^a$

atom	x	y	z	$B_{\text{eq}}, \text{\AA}^2$
P	0.2215(1)	0.01466(7)	0.27821(6)	3.13(2)*
F(1)	-0.0062(3)	0.0309(2)	0.2797(1)	4.18(5)*
F(2)	0.4508(3)	0.0003(2)	0.2884(1)	5.02(6)*
F(3)	0.1953(3)	-0.0030(1)	0.1663(1)	4.15(5)*
O(1)	0.1960(4)	-0.1160(2)	0.2937(2)	4.48(7)*
O(2)	0.2462(4)	0.1452(2)	0.2607(2)	5.49(8)*
N(1a)	0.2582(7)	0.0632(4)	0.4075(4)	2.8(1)*
N(1b)	0.2441(7)	0.0074(4)	0.4191(4)	2.3(1)*
N(2a)	0.2601(7)	0.0128(4)	0.4838(4)	3.1(1)*
N(2b)	0.2722(7)	0.0888(4)	0.4798(3)	2.2(1)*
C(1)	0.1937(5)	-0.1606(3)	0.3822(2)	3.17(9)*
C(2)	0.2247(5)	-0.0965(3)	0.4632(3)	3.06(8)*
C(3)	0.2270(5)	-0.1382(3)	0.5564(3)	4.1(1)*
C(4)	0.1975(5)	-0.2460(3)	0.5656(3)	4.5(1)*
C(5)	0.1644(5)	-0.3103(3)	0.4839(3)	4.1(1)*
C(6)	0.1630(5)	-0.2693(3)	0.3918(3)	3.8(1)*
C(11)	0.2753(5)	0.2172(3)	0.3342(3)	3.70(9)*
C(12)	0.2863(5)	0.1835(3)	0.4291(3)	4.1(1)*
C(13)	0.3167(6)	0.2565(3)	0.5045(3)	5.0(1)*
C(14)	0.3340(5)	0.3628(3)	0.4832(3)	4.6(1)*
C(15)	0.3199(5)	0.3959(3)	0.3878(3)	4.0(1)*
C(16)	0.2917(6)	0.3247(3)	0.3130(3)	4.0(1)*

^a Values for anisotropically-refined atoms are marked with an asterisk. Displacement parameters for the anisotropically refined atoms are given in the form of the equivalent isotropic Gaussian displacement parameter, B_{eq} , defined as $\frac{1}{3}[a^2\beta_{11} + b^2\beta_{22} + c^2\beta_{33} + ab(\cos \gamma)\beta_{12} + ac(\cos \beta)\beta_{13} + bc(\cos \alpha)\beta_{23}]$.

Table 7. Selected Interatomic Distances (\AA) for $\{\text{OC}_6\text{H}_4\text{N}=\text{NC}_6\text{H}_4\text{O}\}\text{PF}_3$

P-F(1)	1.596(2)	N(2b)-C(12)	1.384(8)
P-F(2)	1.588(2)	C(1)-C(2)	1.374(4)
P-F(3)	1.558(2)	C(1)-C(6)	1.379(4)
P-O(1)	1.653(2)	C(2)-C(3)	1.394(4)
P-O(2)	1.656(2)	C(3)-C(4)	1.366(4)
P-N(1a)	1.881(9)	C(4)-C(5)	1.383(4)
P-N(1b)	1.95(1)	C(5)-C(6)	1.378(4)
O(1)-C(1)	1.352(3)	C(11)-C(12)	1.378(4)
O(2)-C(11)	1.354(3)	C(11)-C(16)	1.378(4)
N(1a)-N(2a)	1.23(1)	C(12)-C(13)	1.381(5)
N(1a)-C(12)	1.536(9)	C(13)-C(14)	1.365(5)
N(1b)-N(2b)	1.317(9)	C(14)-C(15)	1.380(4)
N(1b)-C(2)	1.445(9)	C(15)-C(16)	1.362(4)
N(2a)-C(2)	1.405(9)		

In the present study, the non-metallic phosphorus atom is made more electropositive (or acidic) by highly electronegative substituents: F, Cl, or CF_3 . The fluorine atom is undoubtedly the most electronegative substituent of the three and is expected to form the most electronically stable compound. The stronger P-F bond compared with the P-Cl bond is substantiated by analysis of the mass spectra. For example, the mass spectrum of $\{\text{O}(\text{t-Bu})\text{C}_6\text{H}_3\text{N}(\text{CH})\text{C}_6\text{H}_4\text{O}\}\text{PF}_3$ showed only the parent ion and the fragment corresponding to the loss of a CH_3 moiety (confirmed by high resolution mass spectrometry) from the *tert*-butyl group which is subsequently stabilized by conjugation (Figure 2). No species corresponding to the loss of a halogen to form $[\{\text{O}(\text{t-Bu})\text{C}_6\text{H}_3\text{N}(\text{CH})\text{C}_6\text{H}_4\text{O}\}\text{PX}_2]^+$ was observed. In contrast, the Cl- and CF_3 -substituted analogues readily lose one or more of these substituents to form species which often constitute the largest intensity fragments. The mass spectra also show, as demonstrated previously,¹³ that CF_2 is readily eliminated from CF_3P compounds to form species containing P-F bonds.

The ^{19}F and ^{31}P NMR chemical shifts, spin-spin coupling constants and representative NMR spectra are shown in Table

(11) Ramesh, K.; Lal, T. K.; Mukherjee, R. N. *Polyhedron* **1992**, *11*, 3083.
Clague, M. J.; Keder, N. L.; Butler, A. *Inorg. Chem.* **1993**, *32*, 4754.
Dutta, S.; Basu, P.; Chakravorty, A. *Inorg. Chem.* **1993**, *32*, 5343.
(12) Dutta, S.; Chakravorty, A. *Polyhedron* **1994**, *13*, 1811 and references therein.

(13) Cavell, R. G.; Dobbie, R. C. *Inorg. Chem.* **1968**, *7*: (a) 101; (b) 690.

Table 8. Selected Interatomic Angles (deg) for $\{\text{OC}_6\text{H}_4\text{N}=\text{NC}_6\text{H}_4\text{O}\}\text{PF}_3$

F(1)–P–F(2)	174.17(9)	N(2b)–N(1b)–C(2)	115.5(9)
F(1)–P–F(3)	92.7(1)	N(1a)–N(2a)–C(2)	110(1)
F(1)–P–O(1)	90.0(1)	N(1b)–N(2b)–C(12)	110.1(8)
F(1)–P–O(2)	90.0(1)	O(1)–C(1)–C(2)	119.2(2)
F(1)–P–N(1a)	87.4(2)	O(1)–C(1)–C(6)	120.8(3)
F(1)–P–N(1b)	86.5(2)	C(2)–C(1)–C(6)	120.0(3)
F(2)–P–F(3)	93.16(9)	N(1b)–C(2)–C(1)	100.6(4)
F(2)–P–O(1)	90.1(1)	N(1b)–C(2)–C(3)	137.5(4)
F(2)–P–O(2)	90.1(1)	N(2a)–C(2)–C(1)	137.2(4)
F(2)–P–N(1a)	86.9(2)	N(2a)–C(2)–C(3)	101.0(4)
F(2)–P–N(1b)	87.7(2)	C(1)–C(2)–C(3)	121.8(3)
F(3)–P–O(1)	89.47(9)	C(2)–C(3)–C(4)	118.0(3)
F(3)–P–O(2)	89.6(1)	C(3)–C(4)–C(5)	120.1(3)
F(3)–P–N(1a)	169.3(2)	C(4)–C(5)–C(6)	121.9(3)
F(3)–P–N(1b)	169.0(2)	C(1)–C(6)–C(5)	118.1(3)
O(1)–P–O(2)	179.0(1)	O(2)–C(11)–C(12)	120.3(3)
O(1)–P–N(1a)	101.2(2)	O(2)–C(11)–C(16)	119.3(3)
O(1)–P–N(1b)	79.6(2)	C(12)–C(11)–C(16)	120.4(3)
O(2)–P–N(1a)	79.7(2)	N(1a)–C(12)–C(11)	96.9(4)
O(2)–P–N(1b)	101.4(2)	N(1a)–C(12)–C(13)	142.5(4)
P–O(1)–C(1)	122.5(2)	N(2b)–C(12)–C(11)	138.5(4)
P–O(2)–C(1)	123.2(2)	N(2b)–C(12)–C(13)	100.8(4)
P–N(1a)–N(2a)	130(1)	C(11)–C(12)–C(13)	120.7(3)
P–N(1a)–C(12)	119.9(4)	C(12)–C(13)–C(14)	118.8(3)
N(2a)–N(1a)–C(12)	110(1)	C(13)–C(14)–C(15)	120.1(3)
P–N(1b)–N(2b)	126.5(8)	C(14)–C(15)–C(16)	121.7(3)
P–N(1b)–C(2)	118.0(4)	C(11)–C(16)–C(15)	118.4(3)

Table 9. Atomic Coordinates and Equivalent Isotropic Displacement Parameters for $\{[2\text{-O-3,5-(}^t\text{Bu)}_2\text{C}_6\text{H}_2\text{]}_2\text{S}\}\text{PCl}_3^a$

atom	<i>x</i>	<i>y</i>	<i>z</i>	<i>B</i> _{eq} , Å ²
Cl(1)	0.17112(6)	0.15153(6)	−0.05323(4)	3.79(2)*
Cl(2)	0.07042(6)	0.33480(6)	−0.13439(5)	3.62(2)*
Cl(3)	0.27016(5)	0.26474(6)	−0.17247(5)	3.73(2)*
S	0.18759(4)	0.05972(5)	−0.22008(4)	2.16(1)*
P	0.12649(5)	0.20577(5)	−0.17392(4)	2.46(2)*
O(1)	0.1003(1)	0.2431(1)	−0.2707(1)	3.01(5)*
O(2)	0.0203(1)	0.1498(1)	−0.1776(1)	3.03(5)*
C(1)	0.1585(2)	0.0948(2)	−0.3245(2)	2.04(6)*
C(2)	0.1184(2)	0.1878(2)	−0.3360(2)	2.25(6)*
C(3)	0.0966(2)	0.2267(2)	−0.4151(2)	2.28(6)*
C(4)	0.1172(2)	0.1661(2)	−0.4783(2)	2.47(6)*
C(5)	0.1579(2)	0.0723(2)	−0.4681(2)	2.23(6)*
C(6)	0.1797(2)	0.0365(2)	−0.3887(2)	2.21(6)*
C(7)	0.0544(2)	0.3298(2)	−0.4298(2)	2.89(7)*
C(8)	−0.0407(2)	0.3403(2)	−0.3942(2)	4.37(9)*
C(9)	0.0331(3)	0.3528(2)	−0.5217(2)	4.52(9)*
C(10)	0.1291(2)	0.4053(2)	−0.3905(2)	3.99(8)*
C(11)	0.1770(2)	0.0141(2)	−0.5441(2)	2.69(7)*
C(12)	0.2086(3)	−0.0908(3)	−0.5231(2)	5.6(1)*
C(13)	0.2543(3)	0.0658(3)	−0.5843(2)	6.1(1)*
C(14)	0.0842(2)	0.0086(3)	−0.6052(2)	4.8(1)*
C(21)	0.0867(2)	−0.0081(2)	−0.1972(2)	2.25(6)*
C(22)	0.0111(2)	0.0489(2)	−0.1768(2)	2.44(6)*
C(23)	−0.0720(2)	0.0049(2)	−0.1565(2)	2.49(6)*
C(24)	−0.0723(2)	−0.0975(2)	−0.1550(2)	2.79(7)*
C(25)	0.0044(2)	−0.1567(2)	−0.1719(2)	2.48(6)*
C(26)	0.0856(2)	−0.1092(2)	−0.1938(2)	2.36(6)*
C(27)	−0.1579(2)	0.0669(2)	−0.1356(2)	3.11(7)*
C(28)	−0.1282(2)	0.1167(3)	−0.0521(2)	4.69(9)*
C(29)	−0.2469(2)	0.0021(3)	−0.1302(2)	4.16(9)*
C(30)	−0.1887(2)	0.1443(3)	−0.2018(2)	4.24(9)*
C(31)	−0.0006(2)	−0.2693(2)	−0.1704(2)	3.02(7)*
C(32)	−0.0174(3)	−0.3068(3)	−0.2593(2)	4.44(9)*
C(33)	−0.0820(3)	−0.3066(3)	−0.1261(2)	5.0(1)*
C(34)	0.0951(3)	−0.3121(2)	−0.1275(2)	4.6(1)*

^a Values for anisotropically-refined atoms are marked with an asterisk. Displacement parameters for the anisotropically refined atoms are given in the form of the equivalent isotropic Gaussian displacement parameter, *B*_{eq}, defined as $\frac{1}{3}[a^2\beta_{11} + b^2\beta_{22} + c^2\beta_{33} + ab(\cos\gamma)\beta_{12} + ac(\cos\beta)\beta_{13} + bc(\cos\alpha)\beta_{23}]$.

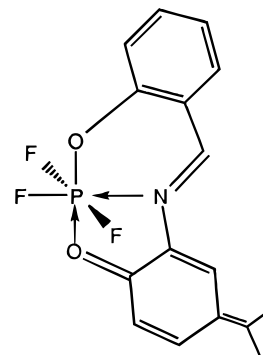
12 and Figures 3–6. The high-field resonances in the ³¹P NMR spectra (δ −36.4 to −148.9 ppm) are indicative of hexacoor-

Table 10. Selected Interatomic Distances (Å) for $\{[2\text{-O-3,5-(}^t\text{Bu)}_2\text{C}_6\text{H}_2\text{]}_2\text{S}\}\text{PCl}_3$

Cl(1)–P	2.1322(9)	C(1)–C(6)	1.387(3)
Cl(2)–P	2.0635(9)	C(2)–C(3)	1.401(3)
Cl(3)–P	2.1608(8)	C(3)–C(4)	1.388(3)
S–P	2.3307(8)	C(4)–C(5)	1.398(3)
S–C(1)	1.778(2)	C(5)–C(6)	1.389(3)
S–C(21)	1.770(2)	C(21)–C(22)	1.390(3)
P–O(1)	1.666(2)	C(21)–C(26)	1.375(3)
P–O(2)	1.662(2)	C(22)–C(23)	1.389(3)
O(1)–C(2)	1.364(2)	C(23)–C(24)	1.391(3)
O(2)–C(22)	1.378(3)	C(24)–C(25)	1.401(3)
C(1)–C(2)	1.386(3)	C(25)–C(26)	1.397(3)

Table 11. Selected Interatomic Angles (deg) for $\{[2\text{-O-3,5-(}^t\text{Bu)}_2\text{C}_6\text{H}_2\text{]}_2\text{S}\}\text{PCl}_3$

P–S–C(1)	92.44(7)	C(2)–C(1)–C(6)	122.9(2)
P–S–C(21)	92.00(7)	O(1)–C(2)–C(1)	120.7(2)
C(1)–S–C(21)	105.32(9)	O(1)–C(2)–C(3)	119.1(2)
Cl(1)–P–Cl(2)	94.26(3)	C(1)–C(2)–C(3)	120.2(2)
Cl(1)–P–Cl(3)	88.08(4)	C(2)–C(3)–C(4)	115.7(2)
Cl(1)–P–S	86.38(3)	C(2)–C(3)–C(7)	121.5(2)
Cl(1)–P–O(1)	174.82(6)	C(4)–C(3)–C(7)	122.8(2)
Cl(1)–P–O(2)	91.17(6)	C(3)–C(4)–C(5)	125.1(2)
Cl(2)–P–Cl(3)	94.30(3)	C(4)–C(5)–C(6)	117.7(2)
Cl(2)–P–S	179.1(1)	C(1)–C(6)–C(5)	118.5(2)
Cl(2)–P–O(1)	90.06(6)	C(8)–C(7)–C(9)	107.4(2)
Cl(2)–P–O(2)	91.36(6)	S–C(21)–C(22)	114.6(2)
Cl(3)–P–S	86.38(3)	S–C(21)–C(26)	122.9(2)
Cl(3)–P–O(1)	88.74(6)	C(22)–C(21)–C(26)	122.4(2)
Cl(3)–P–O(2)	174.34(6)	O(2)–C(22)–C(21)	118.6(2)
S–P–O(1)	89.33(6)	O(2)–C(22)–C(23)	120.9(2)
S–P–O(2)	87.97(6)	C(21)–C(22)–C(23)	120.5(2)
O(1)–P–O(2)	91.58(8)	C(22)–C(23)–C(24)	116.1(2)
P–O(1)–C(2)	123.2(1)	C(23)–C(24)–C(25)	124.5(2)
P–O(2)–C(22)	122.6(1)	C(24)–C(25)–C(26)	117.3(2)
S–C(1)–C(2)	114.3(2)	C(21)–C(26)–C(25)	119.1(2)
S–C(1)–C(6)	122.8(2)		

**Figure 2.** Possible species observed in mass spectra representing $\{\text{O}(^t\text{Bu})\text{C}_6\text{H}_3\text{N}(\text{CH})\text{C}_6\text{H}_4\text{O}\}\text{PF}_3$ with the loss of CH_3 .

dinate phosphorus(V) compounds.^{1–5,14} The ³J_{PH} value (17–27 Hz) in all the Schiff base examples and the ⁴J_{FH} value (2.1 and 2.4 Hz) in $\{\text{O}(^t\text{Bu})\text{C}_6\text{H}_3\text{N}(\text{CH})\text{C}_6\text{H}_4\text{O}\}\text{PF}_3$ and $\{\text{OC}_6\text{H}_4\text{N}=\text{NC}_6\text{H}_4\text{O}\}\text{PF}_3$ respectively (e.g. Figure 6) also confirm the strong coordination of the nitrogen atom. The solid-state NMR spectrum of $\{\text{O}(^t\text{Bu})\text{C}_6\text{H}_3\text{N}(\text{CH})\text{C}_6\text{H}_4\text{O}\}\text{PCl}_3$ shows three species in the six-coordinate phosphorus(V) region {CPMAS ³¹P{¹H} (δ /ppm, (relative intensity), [$\Delta\nu_{1/2}$ /Hz]) −132.2 (2) [ca. 100]; −136.0 (2) [ca. 160]; −148.9 (1) [ca. 900]}. The chemical shift at −136 ppm correlates well with the solution NMR data. Additional resonances are attributed to decomposition products and/or different crystallographic molecular $\{\text{O}(^t\text{Bu})\text{C}_6\text{H}_3\text{N}(\text{CH})\text{C}_6\text{H}_4\text{O}\}\text{PCl}_3$ species (see X-ray structure).

- (14) Cavell, R. G. NMR Studies of the Stereochemistry and Fluxionality of Five and Six Coordinate Phosphorus Compounds. In *Phosphorus-31 NMR Spectroscopy in Stereochemical Analysis*; Verkade, J. G., Quin, L., Eds.; VCH: Deerfield Beach, FL, 1987.

Table 12. NMR Parameters for Hexacoordinate Phosphorus Compounds

compound	chemical shifts ^{a,b} (ppm)				
	³¹ P ^a	¹⁹ F(CF ₃) _{ax}	¹⁹ F(CF ₃) _{rad}	¹⁹ F(PF) _{ax}	¹⁹ F(PF) _{rad}
{O(^t Bu)C ₆ H ₃ N(CH)C ₆ H ₄ O}PCL ₃	-136.4 (1) ^b				
{O(^t Bu)C ₆ H ₃ N(CH)C ₆ H ₄ O}PF ₃	-136.9 (2,3)			-47.7 (2,2)	-75.9 (2,3)
{O(O ₂ N)C ₆ H ₃ N(CH)C ₆ H ₄ O}PF ₃	-137.4 (2,3)			-46.9 (2,2)	-76.4 (2,3)
{OC ₆ H ₄ N=NC ₆ H ₄ O}PF ₃	-143.6 (2,3)			-51.2 (2,2)	-80.0 (2,3)
{OC ₆ H ₄ N(CH)C ₆ H ₄ O}P(CF ₃)F ₂	-144.1 (2,2,4)	-69.3 (2,2,2)		-50.8 (2,2,4)	-76.9 (2,2,4)
{O(^t Bu)C ₆ H ₃ N(CH)C ₆ H ₄ O}P(CF ₃)Cl ₂	-140.6 (4)	-64.3 (2)			
<i>trans</i> -{OC ₆ H ₄ N=NC ₆ H ₄ O}P(CF ₃)F ₂	-148.9 (3,4)		-68.9 (2,3)	-62.1 (2,4)	
<i>cis</i> -{OC ₆ H ₄ N=NC ₆ H ₄ O}P(CF ₃)F ₂	-146.0 (2,2,4)	-69.3 (2,2,2)		-57.7 (2,2,2)	-82.3 (2,2,4)

compound	coupling constants ^c (Hz)									
	¹ J _{PF} ^c		² J _{PF}		³ J _{FF}			³ J _{PH}	⁴ J _{HF} F(ax)	NMR solvent
	ax	rad	ax	rad	² J _{FF}	cis	trans			
{O(^t Bu)C ₆ H ₃ N(CH)C ₆ H ₄ O}PCL ₃								27		CDCl ₃
{O(^t Bu)C ₆ H ₃ N(CH)C ₆ H ₄ O}PF ₃	813	749			47			22	2.1	CDCl ₃
{O(O ₂ N)C ₆ H ₃ N(CH)C ₆ H ₄ O}PF ₃	812	753			46			23	2.4	CD ₃ CN
{OC ₆ H ₄ N=NC ₆ H ₄ O}PF ₃	842	770			47					CD ₃ CN
{OC ₆ H ₄ N(CH)C ₆ H ₄ O}P(CF ₃)F ₂	811	835	125		54	13	3.6	17		CD ₃ CN
{O(^t Bu)C ₆ H ₃ N(CH)C ₆ H ₄ O}P(CF ₃)Cl ₂			144					26		CDCl ₃
<i>trans</i> -{OC ₆ H ₄ N=NC ₆ H ₄ O}P(CF ₃)F ₂	894			134		10				CD ₃ CN
<i>cis</i> -{OC ₆ H ₄ N=NC ₆ H ₄ O}P(CF ₃)F ₂	833	853	128		56	12	4			CD ₃ CN

^a Chemical shift values are given in parts per million (ppm); positive values indicate resonance to high field. ^b Figures in parentheses denote the multiplicity of the resonance. ^c Spin-spin coupling values are given in Hz.

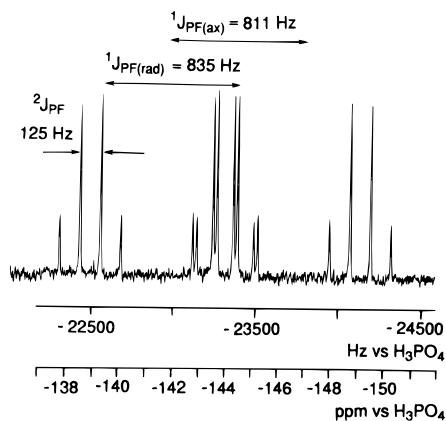


Figure 3. ³¹P{¹H} NMR spectrum (161.98 MHz) of the *cis* isomer (two radial fluorine atoms) of {OC₆H₄N(CH)C₆H₄O}P(CF₃)F₂.

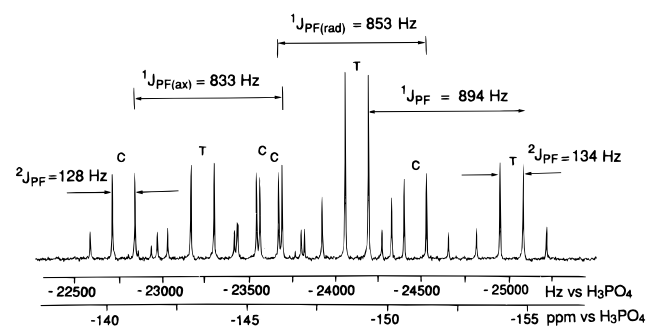


Figure 4. ³¹P{¹H} NMR spectrum (161.98 MHz) of the isomeric mixture of {OC₆H₄N=NC₆H₄O}P(CF₃)F₂. Signal groups labeled C arise from the isomer with two *cis* fluorine atoms and those labeled T arise from the isomer with two *trans* fluorine atoms.

The reaction of some phosphoranes with the unsubstituted Schiff bases (Me₃SiO)C₆H₄N(CH)C₆H₄(OSiMe₃) produced compounds that were often insufficiently soluble for handling, but those which incorporated the *tert*-butyl group (e.g. {O(^tBu)C₆H₃N(CH)C₆H₄O}) gave analogues with increased organic solubility. However, the *tert*-butyl group also increased the possibility for disorder in the molecule, and this has made recrystallization of some {HO(^tBu)C₆H₃N(CH)C₆H₄OH} derivatives very difficult. In these cases the unsubstituted deriva-

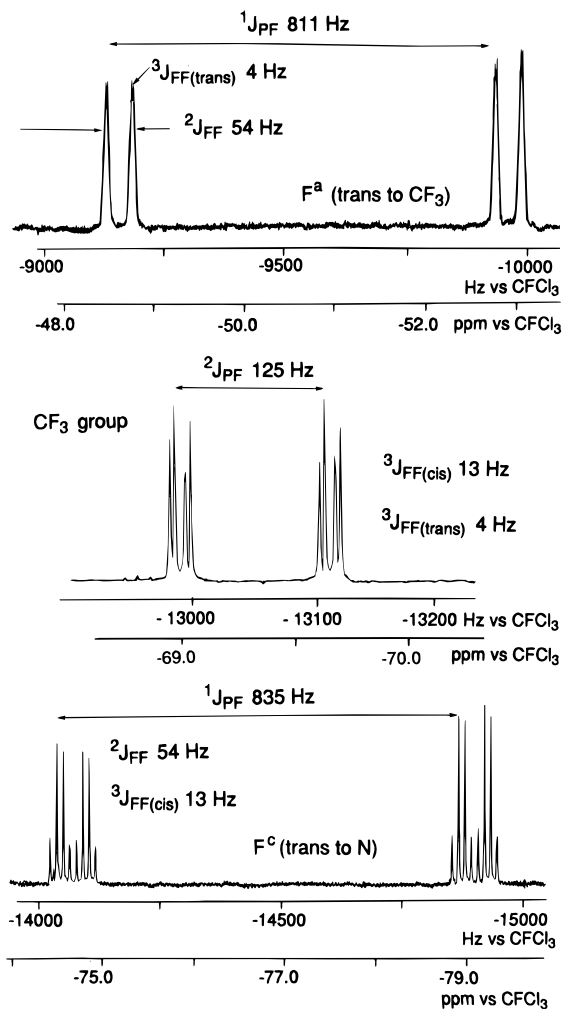


Figure 5. ¹⁹F{¹H} NMR spectrum (188.31 MHz) of the isomer of {OC₆H₄N(CH)C₆H₄O}P(CF₃)F₂ which possesses two *cis*-positioned fluorine atoms.

tives were recrystallized instead. The *tert*-butyl group in {O(^tBu)C₆H₃N(CH)C₆H₄O} may also enhance the ability of tridenticity of the chelate due to its greater donor ability

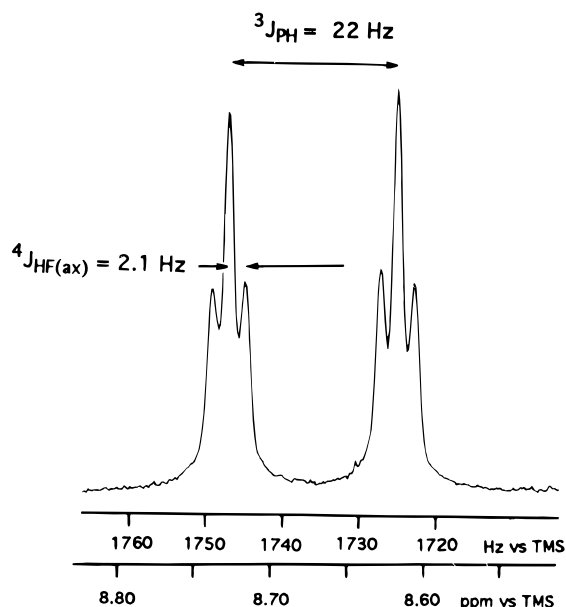


Figure 6. ^1H NMR spectrum (200 MHz) of the C(H) region of $\{\text{OC}_6\text{H}_4\text{N}=\text{NC}_6\text{H}_4\text{O}\}\text{PF}_3$.

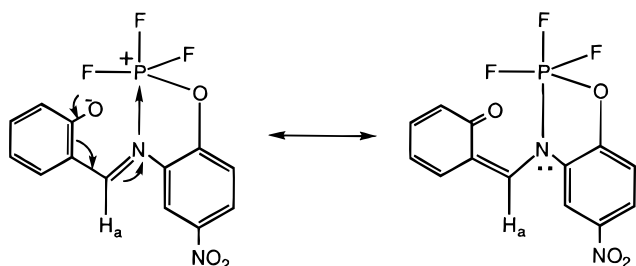


Figure 7. Possible tautomers of $\{\text{O}(\text{O}_2\text{N})\text{C}_6\text{H}_3\text{N}(\text{CH})\text{C}_6\text{H}_4\text{O}\}\text{PF}_3$.

compared to unsubstituted $\{\text{OC}_6\text{H}_4\text{N}(\text{CH})\text{C}_6\text{H}_4\text{O}\}$ derivatives. Conversely, the electron-withdrawing NO_2 substituent in a similar position in $\{\text{O}(\text{O}_2\text{N})\text{C}_6\text{H}_3\text{N}(\text{CH})\text{C}_6\text{H}_4\text{O}\}\text{PF}_3$ significantly decreased the nucleophilicity of the coordinating atoms. Thus, an intermediate pentacoordinate phosphorus(V) species [NMR: ^{31}P , -51 ppm (quart); $^1J_{\text{PF}} = 895$ Hz] was observed during the reaction. The intermediate was stable in solution but was not consistently observed in repeat reactions. The ^1H NMR spectrum [^1H , 6.6 (4H, br, quinoid protons); 7.1 (1H, sharp, s, H_a); 7.9–8.0 (3H, m, aromatic protons on NO_2 ring)] suggests that the species is best assigned to the tautomer corresponding to a quinoidal resonance structure such as that depicted in Figure 7.

During the synthesis of $\{\text{OC}_6\text{H}_4\text{N}=\text{NC}_6\text{H}_4\text{O}\}\text{PF}_3$ an intermediate, $\{\text{Me}_3\text{SiOC}_6\text{H}_4\text{N}=\text{NC}_6\text{H}_4\text{O}\}\text{PF}_4$ which was stable in solution was observed, more consistently if the reaction rate was reduced by not heating the mixture. The ^{31}P NMR spectrum [NMR: δ , -151 ppm (quin); $^1J_{\text{PF}} = 818$ Hz, Figure 8a] suggested that this intermediate corresponded to bidentate chelation of $[\text{Me}_3\text{SiOC}_6\text{H}_4\text{N}=\text{NC}_6\text{H}_4\text{O}]^-$ with preservation of one phenolic O–Si bond. There are two ways for such bidentate $[\text{Me}_3\text{SiOC}_6\text{H}_4\text{N}=\text{NC}_6\text{H}_4\text{O}]^-$ ligation to occur which will form either a five- or a six-membered chelate ring (Figure 9). NMR spectroscopy was unable to distinguish between the isomers. We expect that the inductive effect of the trimethylsilyl group will favor formation of the six-membered ring chelate.

Isomerization is possible for the systems containing one or two CF_3 groups: with one CF_3 group, there is the possibility of axial or radial coordination with respect to the meridional plane formed by the ligand, and with two CF_3 groups, there is the possibility for *cis* or *trans* coordination (Figure 10).

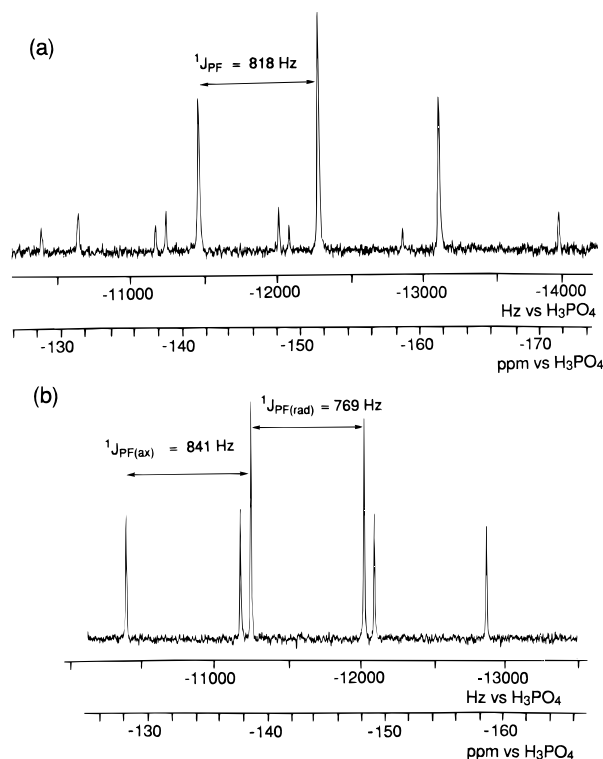


Figure 8. $^{31}\text{P}\{^1\text{H}\}$ NMR spectra (81.015 MHz) of the intermediate (a) and the final six-coordinate product (b) formed from PF_5 and $\text{Me}_3\text{SiOC}_6\text{H}_4\text{N}=\text{NC}_6\text{H}_4\text{OSiMe}_3$.

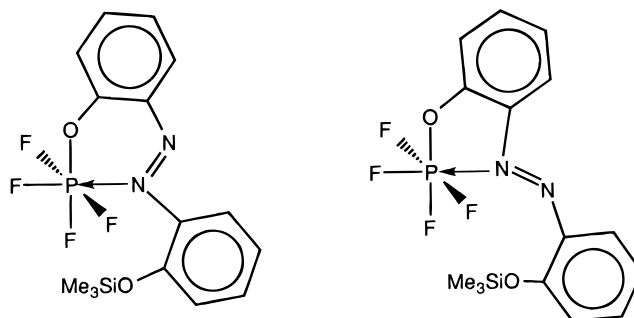


Figure 9. Five- and six-membered rings formed by the bidentate chelation of $[\text{Me}_3\text{SiOC}_6\text{H}_4\text{N}=\text{NC}_6\text{H}_4\text{O}]^-$ in $\{\text{OC}_6\text{H}_4\text{N}=\text{NC}_6\text{H}_4\text{O}\}\text{PF}_3$.

For the *cis* isomers, there is also the possibility of enantiomers but these cannot be differentiated by NMR spectroscopy. The *cis-trans* isomer distribution based only on statistical permutations give a *cis:trans* ratio of 2:1. With the exception of $\{\text{O}(\text{Bu})\text{C}_6\text{H}_3\text{N}(\text{CH})\text{C}_6\text{H}_4\text{O}\}\text{P}(\text{CF}_3)_2\text{Cl}_2$ the P–F spin–spin coupling patterns can reveal these isomerizations in solution.

The ^{19}F and ^{31}P NMR spectra of $\{\text{OC}_6\text{H}_4\text{N}(\text{CH})\text{C}_6\text{H}_4\text{O}\}\text{P}(\text{CF}_3)_2$ (Figures 3 and 5) show an exclusive *cis*- $\{\text{OC}_6\text{H}_4\text{N}(\text{CH})\text{C}_6\text{H}_4\text{O}\}(\text{CF}_3)\text{PF}_2$ conformation for the molecule in solution. In contrast, the ^{19}F and ^{31}P NMR spectra of the crude product, $\{\text{OC}_6\text{H}_4\text{N}=\text{NC}_6\text{H}_4\text{O}\}\text{P}(\text{CF}_3)_2$, shows *ca.* 1:1 ratio of *cis:trans* isomers (Figure 4). Partial separation of isomers was possible by means of fractional recrystallization (*see* Experimental Section). In the case of $\{\text{OC}_6\text{H}_4\text{N}(\text{CH})\text{C}_6\text{H}_4\text{O}\}\text{P}(\text{CF}_3)_2\text{Cl}$, microanalytical data and mass spectra indicate the formation of the compound; however, the interpretation of the ^{19}F and ^{31}P NMR spectra could not be fully assigned. The chemical shift range and spin–spin coupling patterns suggest that we have a molecular neutral six-coordinate $\{\text{OC}_6\text{H}_4\text{N}(\text{CH})\text{C}_6\text{H}_4\text{O}\}\text{P}(\text{CF}_3)_2\text{Cl}$ species in both *cis*- and *trans*-isomeric forms. In addition, two further *cis*- and *trans*-species were observed, and these are tentatively assigned to their

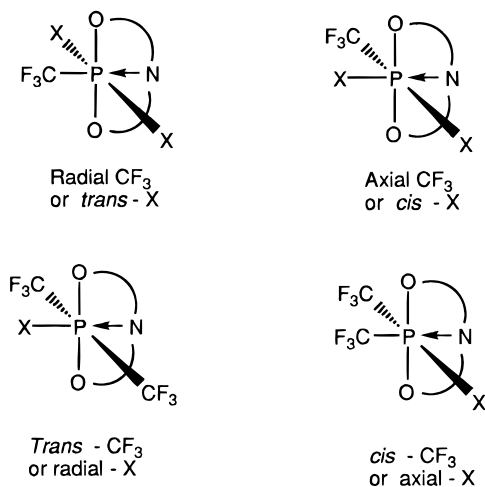


Figure 10. Possible isomeric structures for various $X_x(\text{CF}_3)_{3-x}\text{PL}$ compounds ($x = 1$ or 2 and $X = \text{F}$ or Cl).

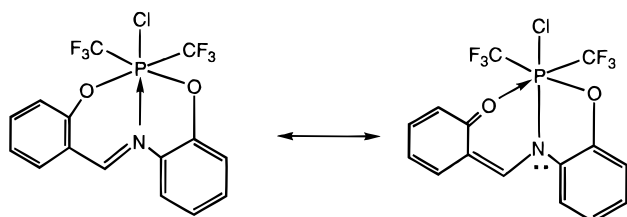


Figure 11. Possible tautomers of $\{\text{OC}_6\text{H}_4\text{N}(\text{CH})\text{C}_6\text{H}_4\text{O}\}\text{P}(\text{CF}_3)_2\text{Cl}$.

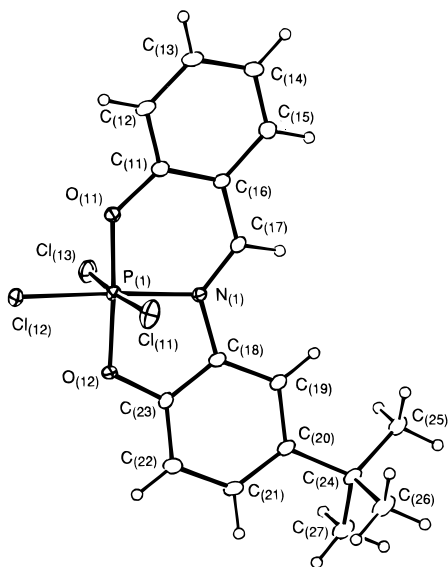


Figure 12. ORTEP¹⁰ view of one of the three $\{\text{O}(\text{tBu})\text{C}_6\text{H}_3\text{N}(\text{CH})\text{C}_6\text{H}_4\text{O}\}\text{PCl}_3$ molecules in the asymmetric unit (the others are essentially identical), showing the atom labeling scheme. Atoms are represented by Gaussian ellipsoids at the 20% probability level, except for hydrogens, which are shown artificially small.

tautomeric forms (Figure 11) on the basis of a similar observed behavior in $\{\text{O}(\text{O}_2\text{N})\text{C}_6\text{H}_3\text{N}(\text{CH})\text{C}_6\text{H}_4\text{O}\}\text{PF}_3$ (Figure 7).

X-ray Structure of $\{\text{O}(\text{tBu})\text{C}_6\text{H}_3\text{N}(\text{CH})\text{C}_6\text{H}_4\text{O}\}\text{PCl}_3$. The structure of $\{\text{O}(\text{tBu})\text{C}_6\text{H}_3\text{N}(\text{CH})\text{C}_6\text{H}_4\text{O}\}\text{PCl}_3$ (Figure 12)¹⁰ shows clearly the six-coordinate environment at the phosphorus center. The coordination geometry of the phosphorus atom is essentially a regular octahedron with the ligand coordinated in the meridional conformation. The compound crystallizes with three independent molecules of $\{\text{O}(\text{tBu})\text{C}_6\text{H}_3\text{N}(\text{CH})\text{C}_6\text{H}_4\text{O}\}\text{PCl}_3$ and half a molecule of acetonitrile per unit cell. Selected bond distances and angles are listed in Tables 4 and 5. All *cis*-O–P–Cl angles are within 2° of the idealized 90° right-

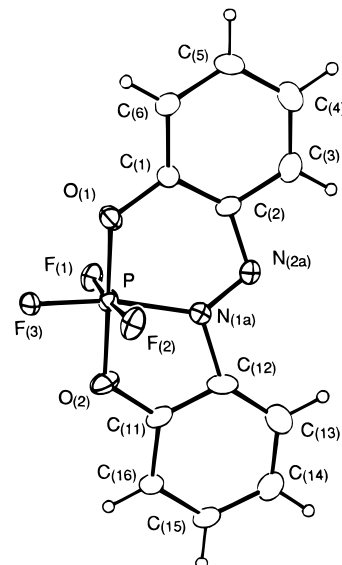


Figure 13. ORTEP¹⁰ view of the $\{\text{OC}_6\text{H}_4\text{N}=\text{NC}_6\text{H}_4\text{O}\}\text{PF}_3$ molecule showing the atom labeling scheme. Atoms are represented by Gaussian ellipsoids at the 20% probability level, except for hydrogens, which are shown artificially small. Only two of the disordered nitrogen atoms are shown.

angle. The largest deviation from 90° is the Cl(13)–P(1)–N(1) angle at 95.4(1)° which forms part of the larger six-membered chelate ring. Both axial chlorine atoms [Cl(11) and Cl(13)] bend very slightly toward the ligand and the Cl(11)–P(1)–Cl(13) angle is 174.03(8)°. The most significant feature of the molecule is the shorter radial chlorine atom (average P–Cl distance of 2.082 Å) compared with the axial chlorine atoms (average P–Cl distance of 2.158 Å). This reflects the relatively weaker dative P–N interaction (average P–N distance of 1.867 Å compares with P–N single bond estimated from covalent radii of 1.78 Å¹⁵) causing a significant *trans* influence on the radial chlorine atom. A similar observation was noted for the analogous $\{(2\text{-methylamino})\text{pyridinato}\}\text{tetrachlorophosphorus(V)}$ molecule where the ring nitrogen atom displayed a similarly longer bond distance to the phosphorus atom reflecting its dative bonding nature and consequently a shorter *trans* P–Cl bond distance.⁵ The P–O bond distances differ slightly for the two different phenolate moieties in favor of a stronger P–O bond for the six-membered chelate ring (average P–O bonds for six- and five-membered chelate rings are 1.641 and 1.674 Å, respectively). This difference of *ca.* 0.03 Å is more pronounced than that of $\text{O}=\text{V}(\text{OEt})(\text{EtOH})\{\text{OC}_6\text{H}_4\text{N}(\text{CH})\text{C}_6\text{H}_4\text{O}\}$ where the difference reported is only *ca.* 0.01 Å.¹¹ The angles about N(1) sum to 359.9°, indicating that this center is planar.

Detailed analysis reveals that the two chelate rings of the ligand lie close to the meridional plane defined by O(11), N(1), O(12), and Cl(12) [dihedral angles for O(11)–P(1)–N(1)–C(18), O(12)–P(1)–N(1)–C(17) and C(18)–N(1)–C(17)–C(16) are +176.62(0.38), +176.73(0.52), and –173.49(0.55)°, respectively] with the two aromatic rings very slightly twisted out-of-plane [dihedral angles for P(1)–O(11)–C(11)–C(12) and P(1)–O(12)–C(23)–C(22) are –170.88(0.45) and +173.62(0.54)°, respectively].

X-ray Structure of $\{\text{OC}_6\text{H}_4\text{N}=\text{NC}_6\text{H}_4\text{O}\}\text{PF}_3$. The structure of $\{\text{OC}_6\text{H}_4\text{N}=\text{NC}_6\text{H}_4\text{O}\}\text{PF}_3$ (Figure 13)¹⁰ shows clearly the six-coordinate environment at the phosphorus center. The coordination geometry of the phosphorus atom is essentially a regular octahedron with the ligand coordinated in the meridional

(15) Pauling, L. *The Nature of the Chemical Bond*, 3rd ed.; Cornell University Press: Ithaca, NY, 1960.

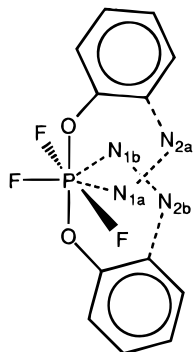


Figure 14. View of the $\{\text{OC}_6\text{H}_4\text{N}=\text{NC}_6\text{H}_4\text{O}\}\text{PF}_3$ molecule illustrating the disorder of the nitrogen atoms. Hydrogen atoms are not shown.

conformation. The positions of the nitrogen atoms of the $\{\text{OC}_6\text{H}_4\text{N}=\text{NC}_6\text{H}_4\text{O}\}$ ligand were found to be disordered and thus were modeled as two half-occupancy pairs, as illustrated in Figure 14.

Selected bond distances and angles are listed in Tables 7 and 8. All *cis*-O–P–F bond angles are within 3° of the idealized 90° right-angle. The main features of the molecule are similar to those reported for $\{\text{O}(\text{tBu})\text{C}_6\text{H}_3\text{N}(\text{CH})\text{C}_6\text{H}_4\text{O}\}\text{PCl}_3$ above. The radial fluorine atom [P–F distance of $1.558(2)$ Å] opposite nitrogen is shorter than that displayed by the axial fluorine atoms (average P–F distance of 1.592 Å) as was the case for the $\{\text{O}(\text{tBu})\text{C}_6\text{H}_3\text{N}(\text{CH})\text{C}_6\text{H}_4\text{O}\}\text{PCl}_3$ molecule described above, and the average P–N bond distance (1.916 Å) is only slightly longer than that found in the same analog.

X-ray Structure of $[\{2\text{-O-3,5-(tBu)}_2\text{C}_6\text{H}_2\}_2\text{S}]\text{PCl}_3$. The thio(bisphenol) derivative, $[\{2\text{-O-3,5-(tBu)}_2\text{C}_6\text{H}_2\}_2\text{S}]\text{PCl}_3$, is similarly a strongly bonded six-coordinated phosphorus(V) derivative (Figure 15) except that, in contrast to the imine and azo compound structures described above, the molecule adopts a *fac* coordination presumably in part influenced by the fact that two five-membered rings must be formed thus the ligand may not be so readily able to span three meridional positions. The bond distances and angles are given in Tables 10 and 11. The P–S bond distance herein 2.331 is the shortest yet observed for this P–S internal coordination and approaches the single bond distance¹⁵ of approximately 2.10 Å and the sum of single bond covalent radii (2.14 Å) for phosphorus and sulfur.¹⁵

The smallest internal P–S coordination bond distance previously reported was 2.36 Å given by Holmes *et al.*^{6a} for a closely related molecule which differs from ours only insofar as we have a Cl on phosphorus in place of their OCH_2CF_3 substituents. We attribute the shortening of this P–S bond to a reduction of steric interaction between the *tert*-butyl groups and the $\text{OCH}_2\text{-CF}_3$ substituents on phosphorus which was present in their compound. It would be interesting to see if an unsubstituted thiodiphenyl ring attached to our system would slip to the *anti* position when steric interactions are reduced as suggested by Holmes,^{6a} in our systems, we have no bulky groups on phosphorus.

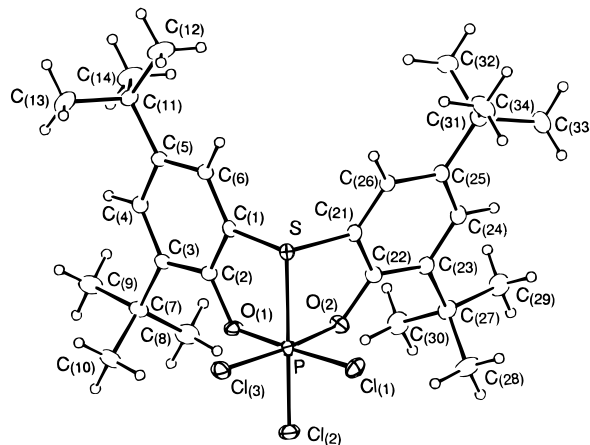


Figure 15. ORTEP¹⁰ view of the $[\{2\text{-O-3,5-(tBu)}_2\text{C}_6\text{H}_2\}_2\text{S}]\text{PCl}_3$ molecule showing the atom labeling scheme. Atoms are represented by Gaussian ellipsoids at the 20% probability level, except for hydrogens, which are shown artificially small.

Conclusion

A new series of neutral hexacoordinate phosphorus compounds containing tridentate ligands has been characterized. The Schiff base and diazo ligands chelate in a meridional conformation forming both a five- and a six-membered chelate ring. The high-field ^{31}P NMR chemical shifts in all cases are characteristic for hexacoordination. The X-ray structures of $\{\text{O}(\text{tBu})\text{C}_6\text{H}_3\text{N}(\text{CH})\text{C}_6\text{H}_4\text{O}\}\text{PCl}_3$, $\{\text{OC}_6\text{H}_4\text{N}=\text{NC}_6\text{H}_4\text{O}\}\text{PF}_3$ and $[\{2\text{-O-3,5-(tBu)}_2\text{C}_6\text{H}_2\}_2\text{S}]\text{PCl}_3$ confirm a slightly distorted octahedral phosphorus(V) center. The thiobisphenol ligand forms a *fac* six-coordinate bischelate and shows the strongest internal coordination interaction (evaluated by bond length) yet observed between P and S in this type of molecule. There are intriguing contrasts and parallels to a related series of trifluoroethoxy P(V) compounds. The possibility for multidenticity in these type of ligands has increased the stability of some intermediates allowing for possible mechanistic analysis. The CF_3 -substituted analogs continue to provide different isomers based on subtle overlapping steric and electronic effects.

Acknowledgment. We thank the Natural Science and Engineering Research Council of Canada for financial support and an International Postdoctoral Fellowship to C.Y.W.

Supporting Information Available: Tables S1-1–S1-8, S2-1–S2-8, and S3-1–S3-8, listing experimental details of the structure determinations, complete positional and thermal parameters, derived hydrogen positions, and complete bond distances and angles and tables of atomic planes are provided for each molecular structure (47 pages). Ordering information is given on any current masthead page.

IC9507530